PICO: Probe of Inflation and Cosmic Origins
Capabilities of a next generation $1B CMB space mission

Elisa Russier

For the PICO collaboration

Cosmic inflation and the search for primordial gravitational waves

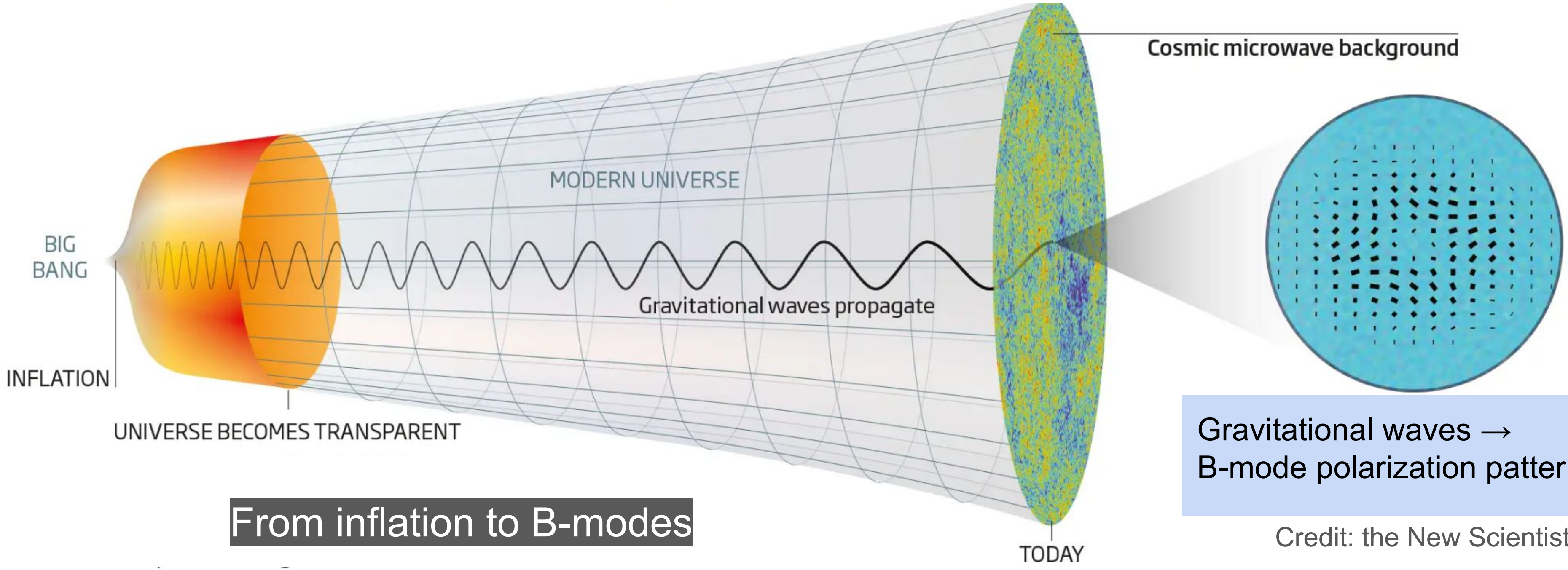

Gravitational waves → B-mode polarization pattern

From inflation to B-modes

Credit: the New Scientist

Inflation key observable

r = T/S

Simplest inflation models → $r \gtrsim 0.001$ ⇒ Study $r = 0$ and $r = 0.003$

Polarization E- and B-modes power spectra

arXiv:1902.10541 **[astro-ph.IM]**

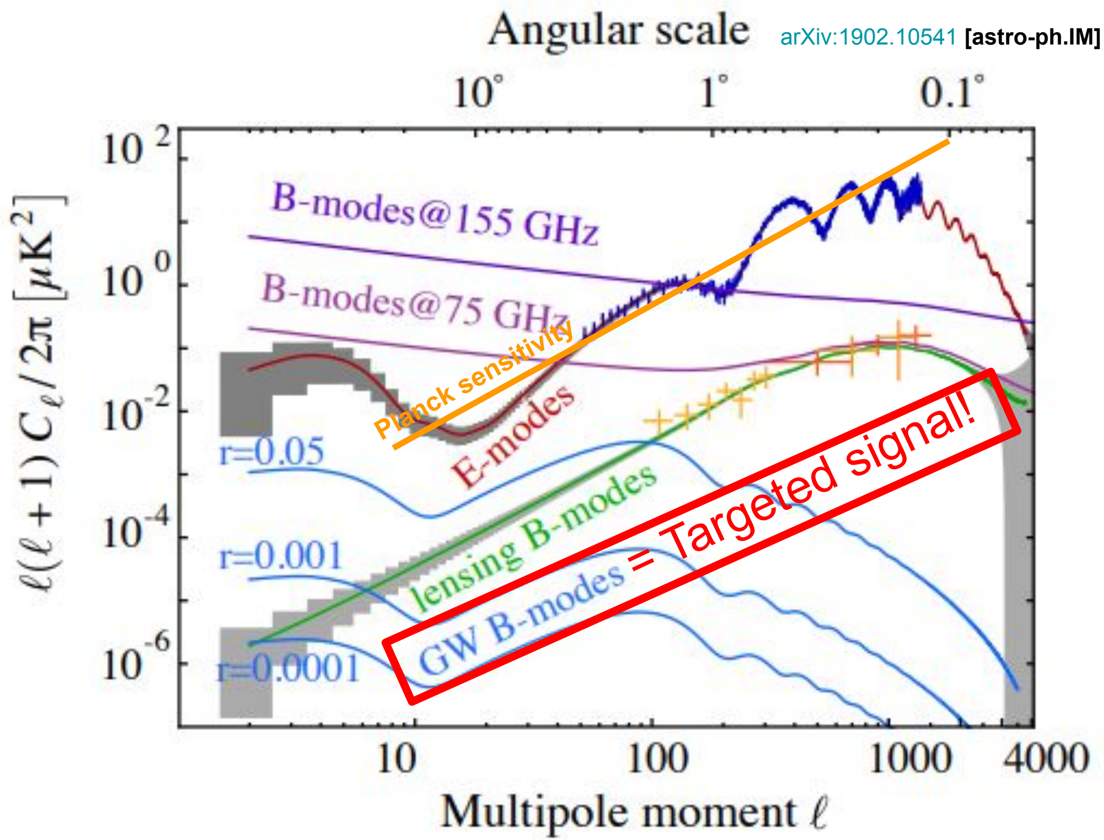

Credit: Sky & Telescope

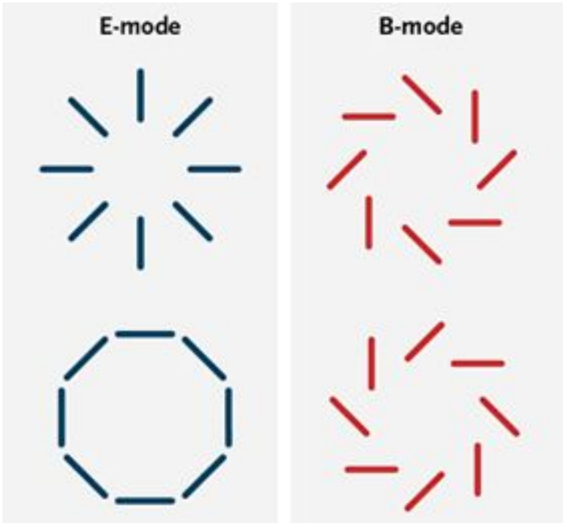

Polarization patterns

Polarization E- and B-modes power spectra

arXiv:1902.10541 **[astro-ph.IM]**

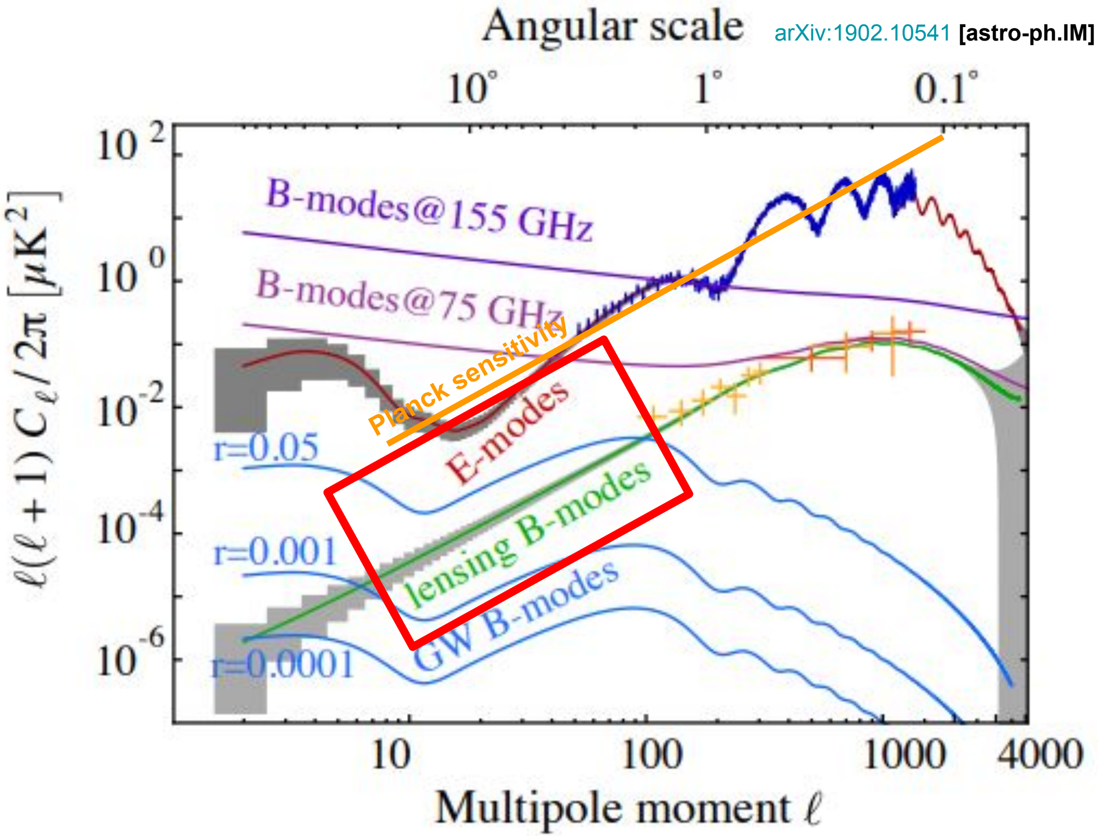

Credit: ESA

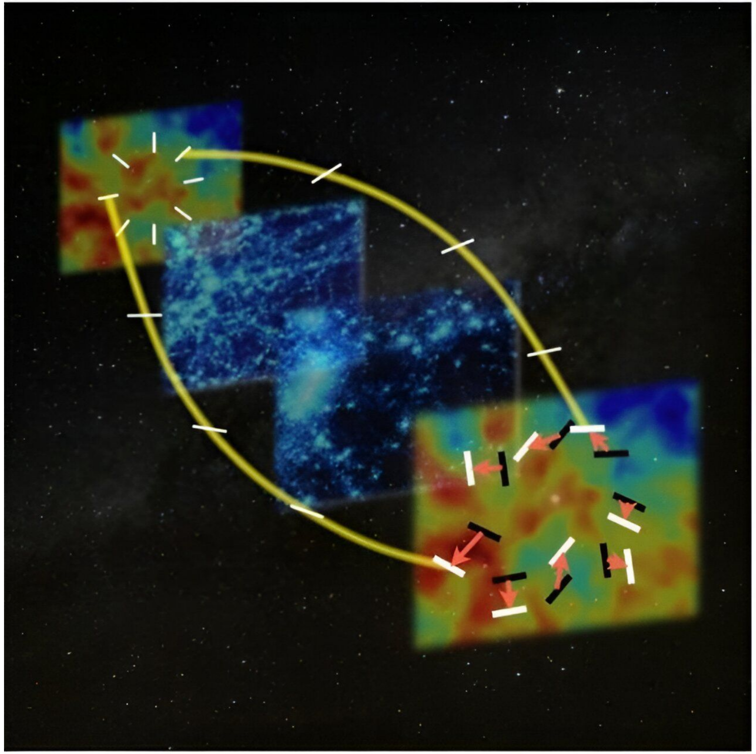

CMB lensing

Polarization E- and B-modes power spectra

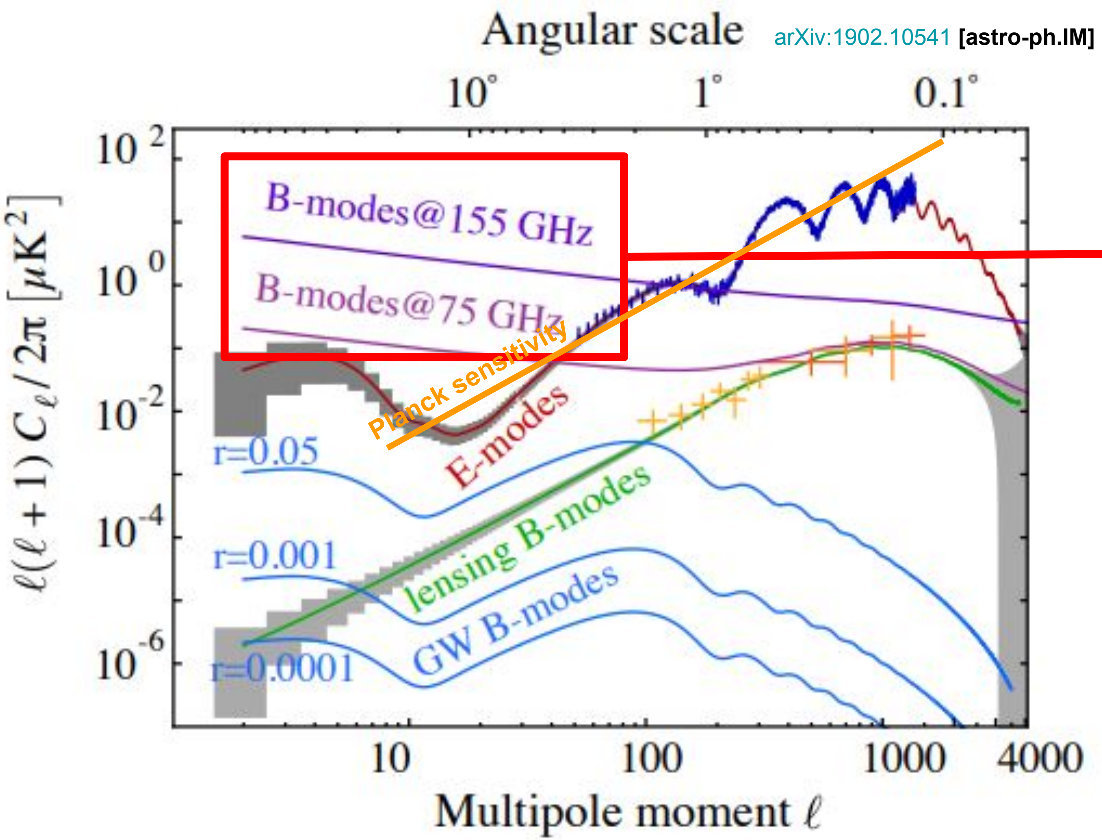

Total B modes:
Large contribution from **foregrounds**!

Sources of contamination: Polarized foregrounds

Credit: F. Bouchet

Our own Galaxy also emits in the CMB observations range!

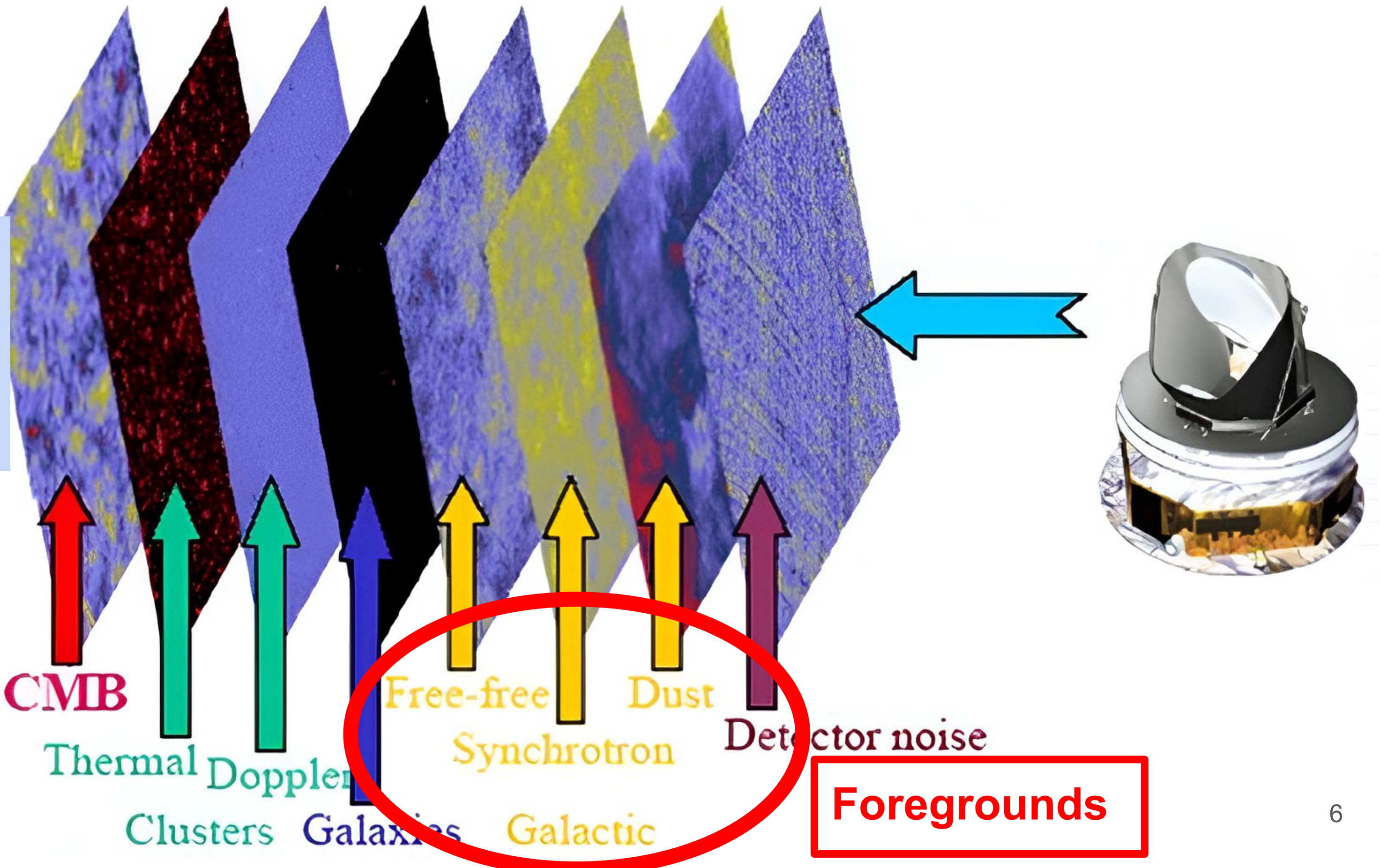

Foregrounds

PICO: Probe of Inflation and Cosmic Origins

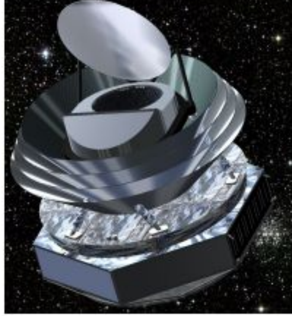

- Most sensitive instrument proposed for the next generation of space missions

  e.g.: It would take ~10000 Planck years to reach PICO's sensitivity!

- Large frequency range and high sensitivity, which can only be achieved with space missions

CMB space missions: Polarization	Planck	Litebird	PICO
Noise sensitivity [μK.arcmin]	52 → (24 x better)	2.16 → (3.5 x better)	0.61
Frequency range [GHz]	30 — 353	34 — 448	21 — 799
Angular resolution [arcmin]	30 — 4.9	70.5 — 17.9	38.4 — 1.1

Large frequency range, high sensitivity, high resolution

Table: CMB space missions sensitivity, frequency and angular resolution range

Foregrounds dominate the inflationary signal!

Foregrounds are orders of magnitude above the inflationary signal!

Large range of frequencies to remove and better characterize the foregrounds:
PICO: 21 GHz to 799 GHz

Goal: Assess whether PICO can achieve foreground cleaning such that the level of constraint on r can be attained

PICO r goal:
if r = 0, 5σ confidence level for r < 5 x 10^{-4}
5σ detection for r = 5 x 10^{-4}

B-mode power spectra for 46% of the sky

JCAP **06** (2023) 034

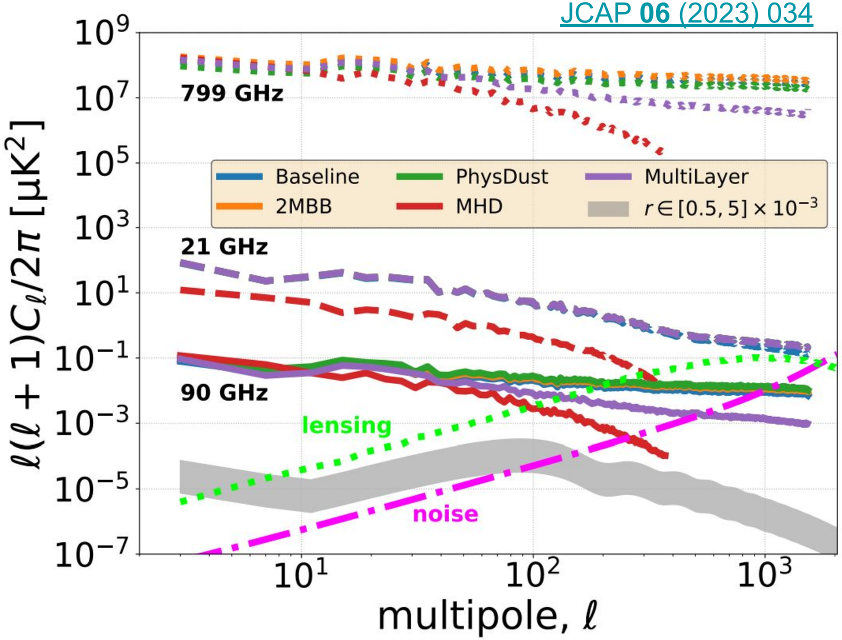

Foregrounds dominate for all frequency bands !!!!

Methodology: How to obtain CMB B mode maps?

Component separation: Blind method: NILC: Needlet Internal Linear Combination
A&A 493, 835-857 (2009)

CMB lensed B mode map

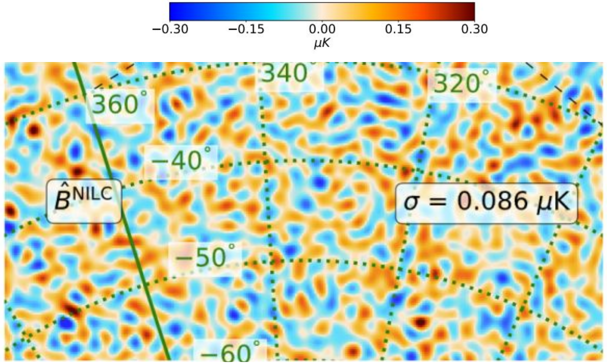

Delensing: Optimal method: Iterative lensing reconstruction on map-level
Sebastian Belkner *et al* 2024 *ApJ* 964 148

CMB delensed B mode map

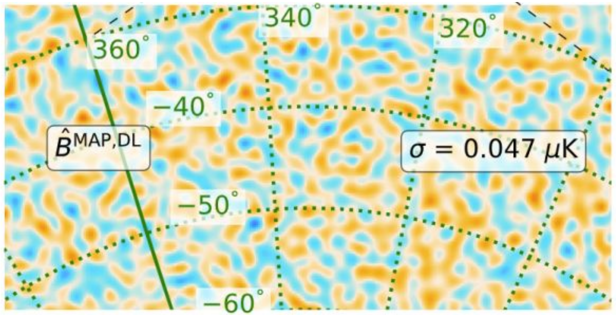

Results: PICO r constraints for different sky models

r = 0 and r = 0.003 after 73% delensing

JCAP **06** (2023) 034

Sky model	r = 0: $r_{95\%}$	r = 0.003: $[r \pm \sigma(r)]$	
Planck Baseline: dust + sync	2.6×10^{-4}	$(3.15 \pm 0.16) \times 10^{-3}$	✓
Two component dust model + sync + AME	1.5×10^{-4}	$(3.09 \pm 0.13) \times 10^{-3}$	✓
Physical Dust + sync + AME	1.3×10^{-4}	$(3.09 \pm 0.11) \times 10^{-3}$	✓
Tigress MHD simulation (dust, sync) + AME	2.7×10^{-4}	$(3.09 \pm 0.11) \times 10^{-3}$	✓
Multi-Layer Dust + sync + AME	13.2×10^{-4}	$(3.93 \pm 0.32) \times 10^{-3}$	✗

r = 0.003
Recover input r value with ~ 20σ confidence
→Strongest for any proposed instrument

⇒ 3σ bias

Why is it biased for the Multi-Layer Dust?
→ Foreground residuals
→ Full sky: some patches of sky more contaminated than others → Multipatch analysis

Multipatch analysis

- MultiLayer sky model: Biased estimation of r
- Mitigation of the bias → compare independent

constraints on r from independent sections of the sky

Equal area sky sections with fsky = 2.5%

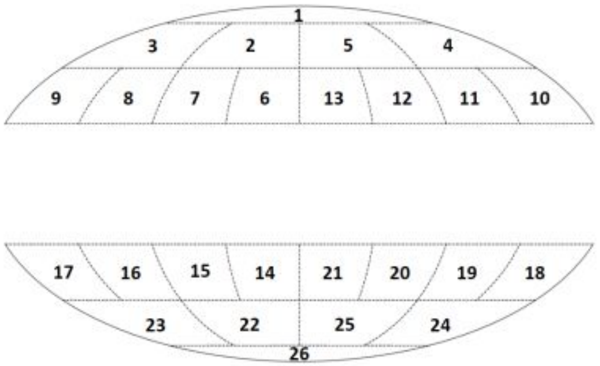

JCAP **06** (2023) 034

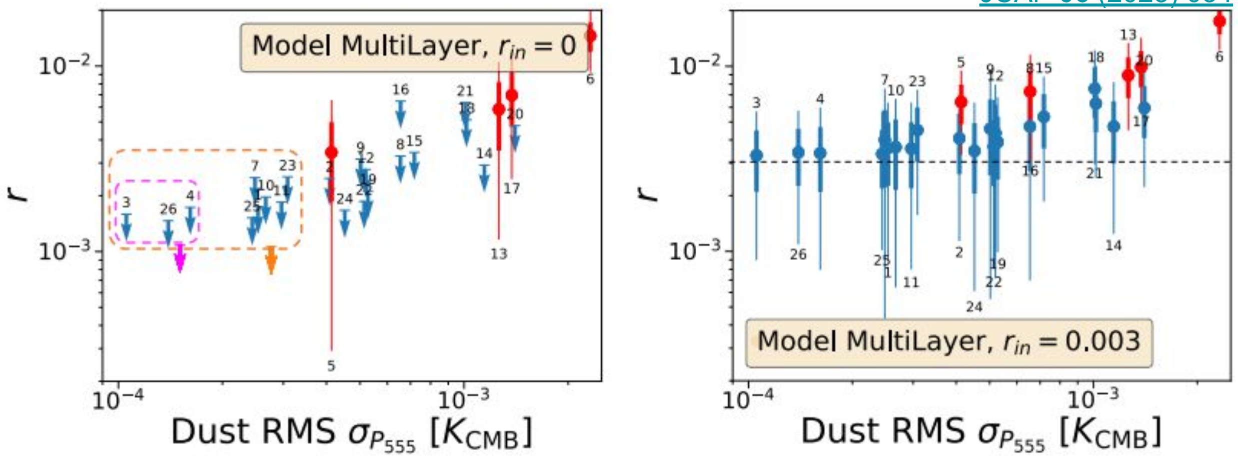

95% confidence limits for r = 0 and r = 0.003 per patch

- Dust → Bias
- Tracer of dust: 555 GHz
- Least contaminated patches:
  For r = 0, $r_{95\%}$ = 1.9x10^{-3} (magenta) $r_{95\%}$ = 1.6x10^{-3} (orange)

⇒ Need a space mission with high sensitivity

My current project

- Published results assume white noise and uniform coverage
- Goal: Assess the effect of 1/f noise and realistic noise sky coverage

Parameters of the mission

- 5 years
- 90% detector operability
- 95% survey efficiency

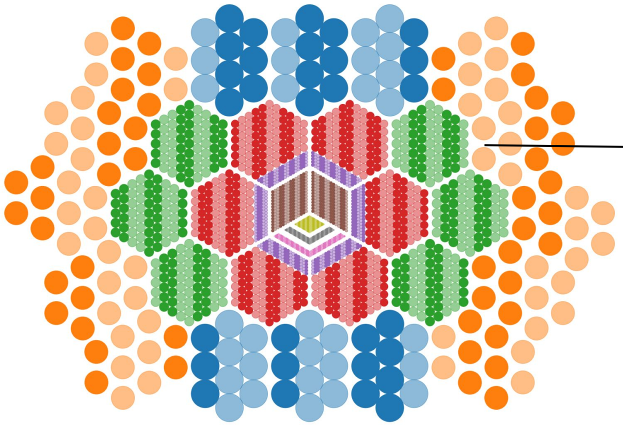

PICO focal plane

Time-Ordered Data with 1/f: 20 mHz

Spin + precession scan strategy

Hits map at 155 GHz

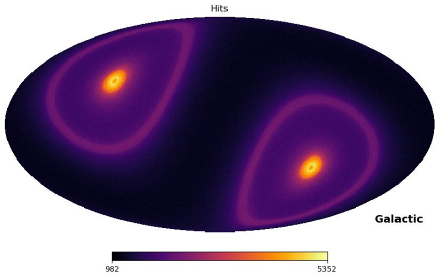

1/f vs white noise

B-mode power spectra at 155 GHz

$Cl_{BB} [\mu K_{CMB}^2]$

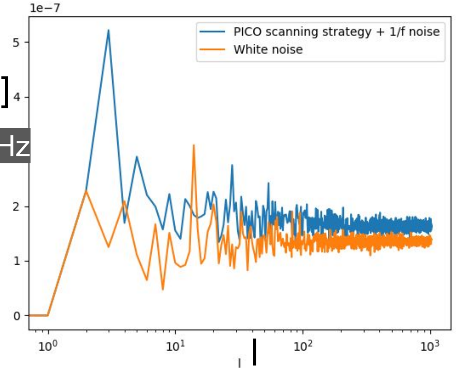

Conclusion: PICO's capabilities

Foregrounds are a major issue in current CMB observations!

For ⅘ sky models:

- if r = 0, rule out simplest models of inflation
- if r = 0.003, detected with confidence levels ~ 20σ after 5 years of mission

High complexity sky model: mitigation of bias

⇒ Strongest upper limits and detection predicted for any instrument

⇒ Need of a space mission to do this with a large frequency range, high resolution and high sensitivity as PICO!

Current work: assess the impact of a more realistic noise on r constraints

ANNEX

PICO mission parameters

Table 1.1: **Mission Parameters**

Combined polarization map depth (rms noise in 1×1 arcmin^2 pixel):	
Baseline	0.87 μK_{CMB} arcmin equivalent to 3300 *Planck* missions
CBE[a]	0.61 μK_{CMB} arcmin equivalent to 6400 *Planck* missions
Survey duration	5 yrs
Orbit type	Sun-Earth L2
Launch mass	2147 kg
Total power	1320 W
Data rate	6.1 Tbits/day
Cost	$ 958M

[a] CBE = Current best estimate.

PICO focal plane

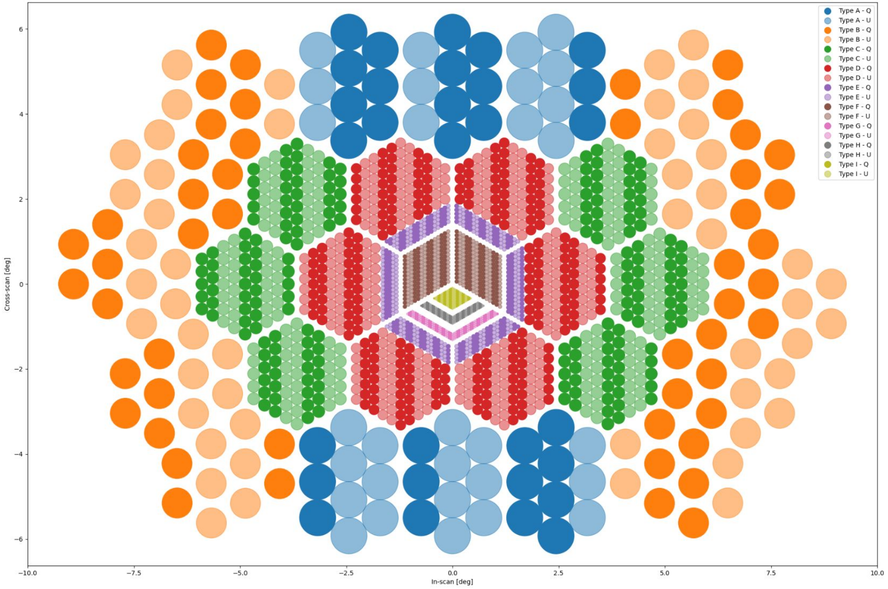

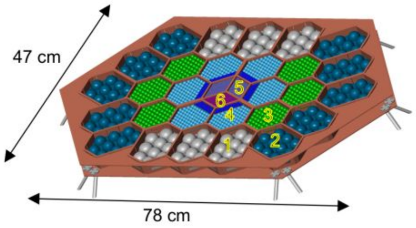

Figure 3.3: PICO focal plane. Detectors are fabricated on six types of tiles (shown numbered and colored as in Table 3.1). The wafers are located on the focal plane such that higher frequency bands, which require better optical performance, are placed nearer to the center. All detectors are within the diffraction-limited performance for their respective frequency bands.

Table 3.1: PICO makes efficient use of the focal area with multichroic pixels (three bands per pixel, § 3.2.1). The sampling rate is based on the smallest beam (Table 3.2), with 3 samples per FWHM at a scan speed $(360°/\mathrm{min})\sin(\beta = 69°) = 336°/\mathrm{min}$. Scaling from suborbital experience, we anticipate that TES bolometers can support these sampling rates with $\sim 4\times$ margin.

Tile type	N_{tile}	Pixels/ tile	Pixel type	Band centers [GHz]	Sampling rate [Hz]
1	6	10	A	21, 30, 43	45
2	10	10	B	25, 36, 52	55
3	6	61	C	62, 90, 129	136
4	6	85	D	75, 108, 155	163
		80	E	186, 268, 385	403
5	2	450	F	223, 321, 462	480
6	1	220	G	555	917
		200	H	666	
		180	I	799	

NILC component separation method

Blind method: No assumption on the spectral dependence of the foregrounds

Use statistical independence between emission of different physical origins

Q, U → almE, almB →

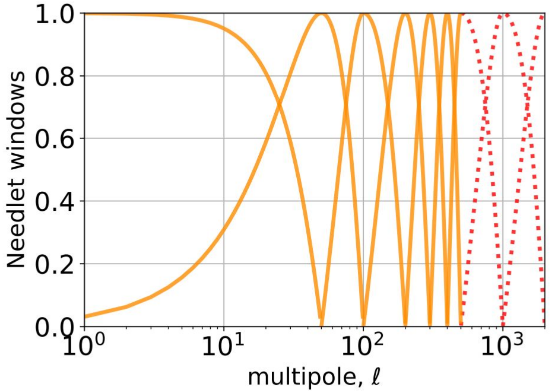

$$\hat{s}^{(j)} = \sum_{\nu} w_{\nu}^{(j)} \, d_{\nu}^{(j)} ,$$

using the specific weights

$$w_{\nu}^{(j)} = \frac{\sum_{\nu'} \mathrm{C}^{-1}{}^{(j)}_{\nu\nu'} \, a_{\nu'}}{\sum_{\nu'} \sum_{\nu''} a_{\nu'} \, \mathrm{C}^{-1}{}^{(j)}_{\nu'\nu''} \, a_{\nu''}} .$$

← Combine each CMB B mode map for each scale

Impact of the low and high frequency channels on r constraint

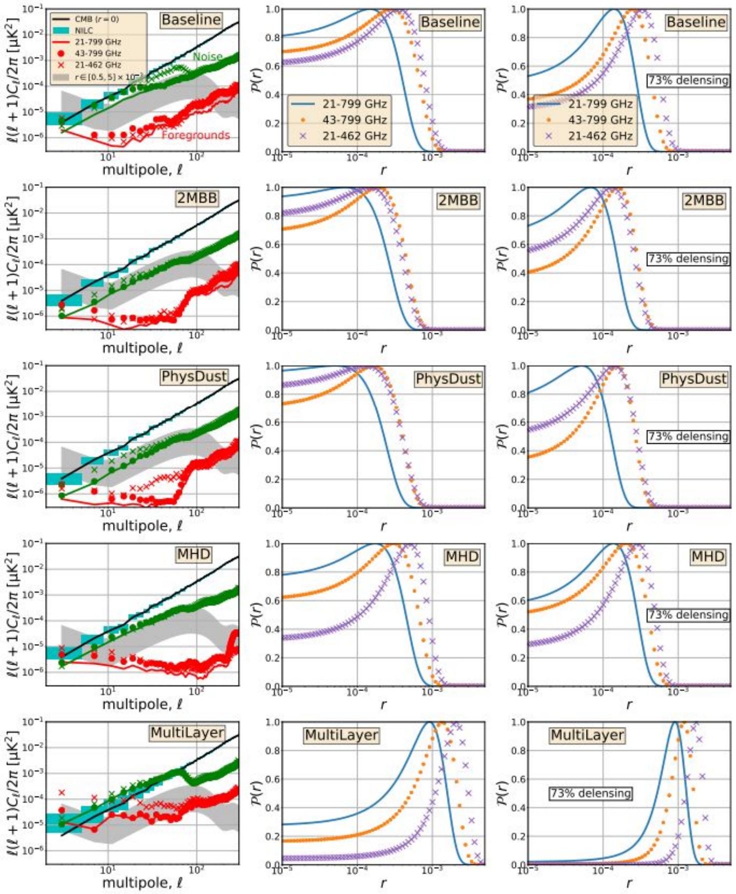

$r_{\rm in} = 0$, 73% delensing				
	PICO-HF (43-799 GHz)		PICO-LF (21-462 GHz)	
Model	$r_{95\%}/10^{-4}$	$r/\sigma(r)$	$r_{95\%}/10^{-4}$	$r/\sigma(r)$
Baseline	4.3	1.5	5.6	1.6
2MBB	2.8	1.4	2.5	1.3
PhysDust	2.6	1.7	2.7	1.3
MHD	3.8	1.3	4.8	1.6
MultiLayer	16.7	3.4	22.8	4.4

Table 4. NILC r forecasts with $r_{\rm in} = 0$ and without either the low frequencies (LF) or the high frequencies (HF), and assuming 73% delensing.

Foreground models part 1

Model Name (Short Name)	Dust Model	Synchrotron Model	Other Components
Planck Baseline (Baseline)	PySM d1: modified black-body with spatially varying T_d and β_d	PySM s1: power law spectrum with spatially varying β_s	None
Dust: Two Modified Black Bodies (2MBB)	PySM d4: two component dust model of [23]	PySM s3: power law spectrum with spatially varying β_s and sky-constant curvature	PySM a2 AME model: Spatially varying spectrum with fixed 2% polarization fraction

Based on Planck 353/WMAP 23 GHz Q, U maps obtained within the Commander framework
Added Gaussian fluctuations at l > 69
lmax = 1500

2 component dust model: combination of Planck and DIRBE/IRAS data + synchrotron with curvature term to the frequency scaling + AME component

Foreground models part 2

Physical Dust (Phys-Dust)	PySM d7: physical dust model of [24] including magnetic dipole emission	PySM s3	PySM a2 AME model
MHD (MHD)	Modified blackbody dust emission in each cell of a TIGRESS MHD simulation [25, 26], integrated along the line of sight	Power law synchrotron spectrum with amplitude coupled to B-fields in a TIGRESS MHD simulation [25, 26]	None

Same as MBB except for dust model: based on physical model of interstellar grains with a distribution of sizes and temperatures

Based on TIGRESS MHD simulations → only dust and synchrotron

Foreground models part 3

Multi-Layer Dust (MultiLayer)	"MKD" dust model [27] based on multiple modified blackbody emission laws in each pixel	PySM s3	PySM a2 AME model

$$Q_\nu^{\mathrm{MKD}} = \sum_k A_{d,k}^Q \left(\frac{\nu}{\nu_0}\right)^{\beta_{d,k}} B_\nu\left(T_{d,k}\right)$$

$$U_\nu^{\mathrm{MKD}} = \sum_k A_{d,k}^U \left(\frac{\nu}{\nu_0}\right)^{\beta_{d,k}} B_\nu\left(T_{d,k}\right)$$

Introduces frequency decorrelation

If parameters describing the frequency scaling of dust emission varies across the sky, they must also vary align the LOS → LOS frequency decorrelation

Input map → NILC CMB B mode map and Residuals

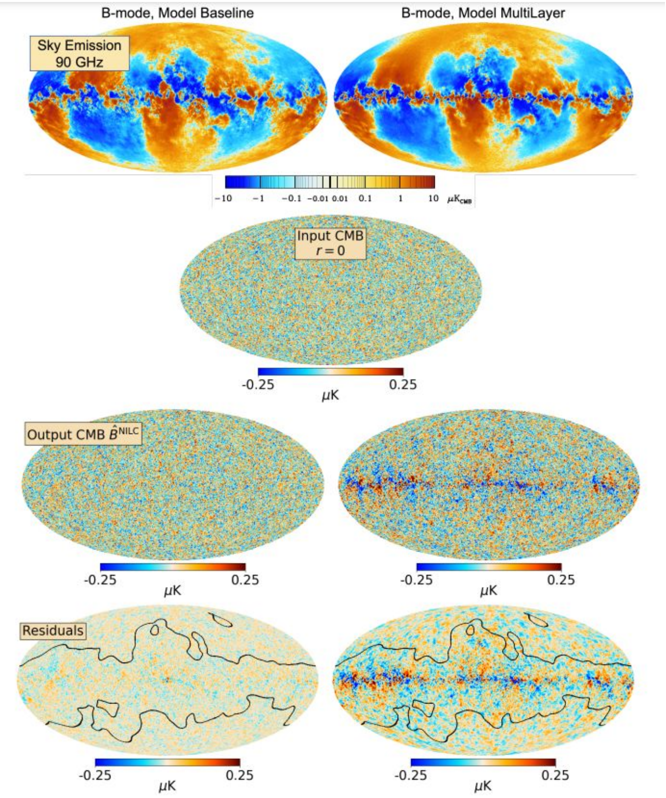

Figure 3. B-mode maps smoothed to 40' fwhm for models Baseline (left) and MultiLayer (right) before and after component separation with NILC. From top to bottom: sky map at 90 GHz; the input CMB with $r = 0$; the output CMB after component separation; and the CMB residual map = output CMB - input CMB, and outline of the 50% mask that determines the portion the sky for power spectra calculations.

Why 73% delensing?

$C_\ell \equiv C_\ell(r, A_{\rm lens}) = rC_\ell^{\rm tens} + A_{\rm lens}C_\ell^{\rm lens}$ with $1 - A_{\rm lens}$ as the delensing factor

With post component separation noise power spectra, use forecasting approach to obtain expected delensed level of the lensing B-mode spectrum

Compute iteratively the quadratic estimator-based lensing noise and then the B mode power spectra after delensing with the associated lensing map

ILC Assumptions	Map Noise Level (μK arcmin) 0.87	0.61
No foregrounds	0.80	0.85
No deprojection; standard ILC	0.80	0.84
Polarized dust deprojected	0.80	0.84
Polarized synchrotron deprojected	0.73	0.78
Polarized dust & synchrotron deprojected	0.73	0.78

Table 5. Forecast delensing factor $1-A_{\rm lens}$ with two map noise levels for different ILC analysis assumptions [20, 57]. The delensing factor is defined in equation (A.5).

Survey strategy + 1/f noise

PICO employs a highly repetitive scan strategy to map the full sky. During the survey, PICO spins with a period $T_{spin} = 1$ min about a spin axis oriented $\alpha = 26^\circ$ from the anti-solar direction (Fig. 4.2). This spin axis is forced to precess about the anti-solar direction with a period $T_{prec} = 10$ hr. The telescope boresight is oriented at an angle $\beta = 69^\circ$ away from the spin axis (Fig. 3.1). This β angle is chosen such that $\alpha + \beta > 90^\circ$, enabling mapping of all ecliptic latitudes. The precession axis tracks along with the Earth in its yearly orbit around the Sun, so this scan strategy maps the full sky (all ecliptic longitudes) within 6 months.

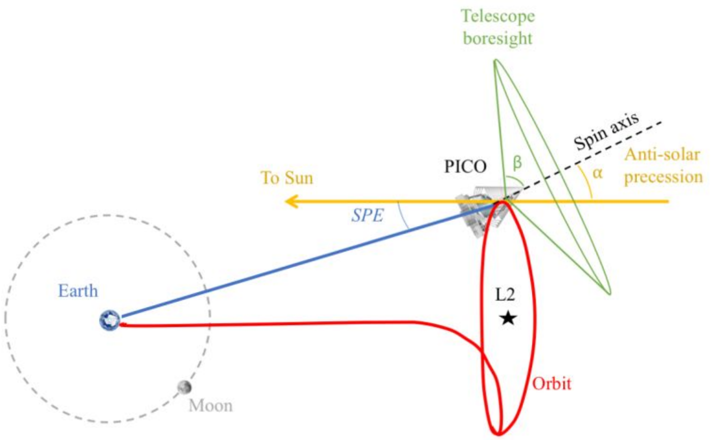

Figure 4.2: PICO surveys by continuously spinning the instrument about a precessing axis.

above the knee in the detector low-frequency noise (§ 3.2.4). A destriping mapmaker applied in data post-processing effectively operates as a high-pass filter, as demonstrated by *Planck* [291]. PICO's spin-axis precession frequency is more than 400 times faster than that of *Planck*, greatly reducing the effects of any residual $1/f$ noise by spreading the effects more isotropically across pixels.

How to generate 1/f noise?

$$P(f) = \frac{\sigma^2}{f_{\mathrm{sample}}} \cdot \frac{f_{\mathrm{min}}^{\alpha} + f^{\alpha}}{f_{\mathrm{knee}}^{\alpha} + f^{\alpha}},$$

Noise spectral density

We generate a realization of the noise first in Fourier space by drawing a vector of random complex numbers. scale them with the noise model and inverse FFT to get a noise realization

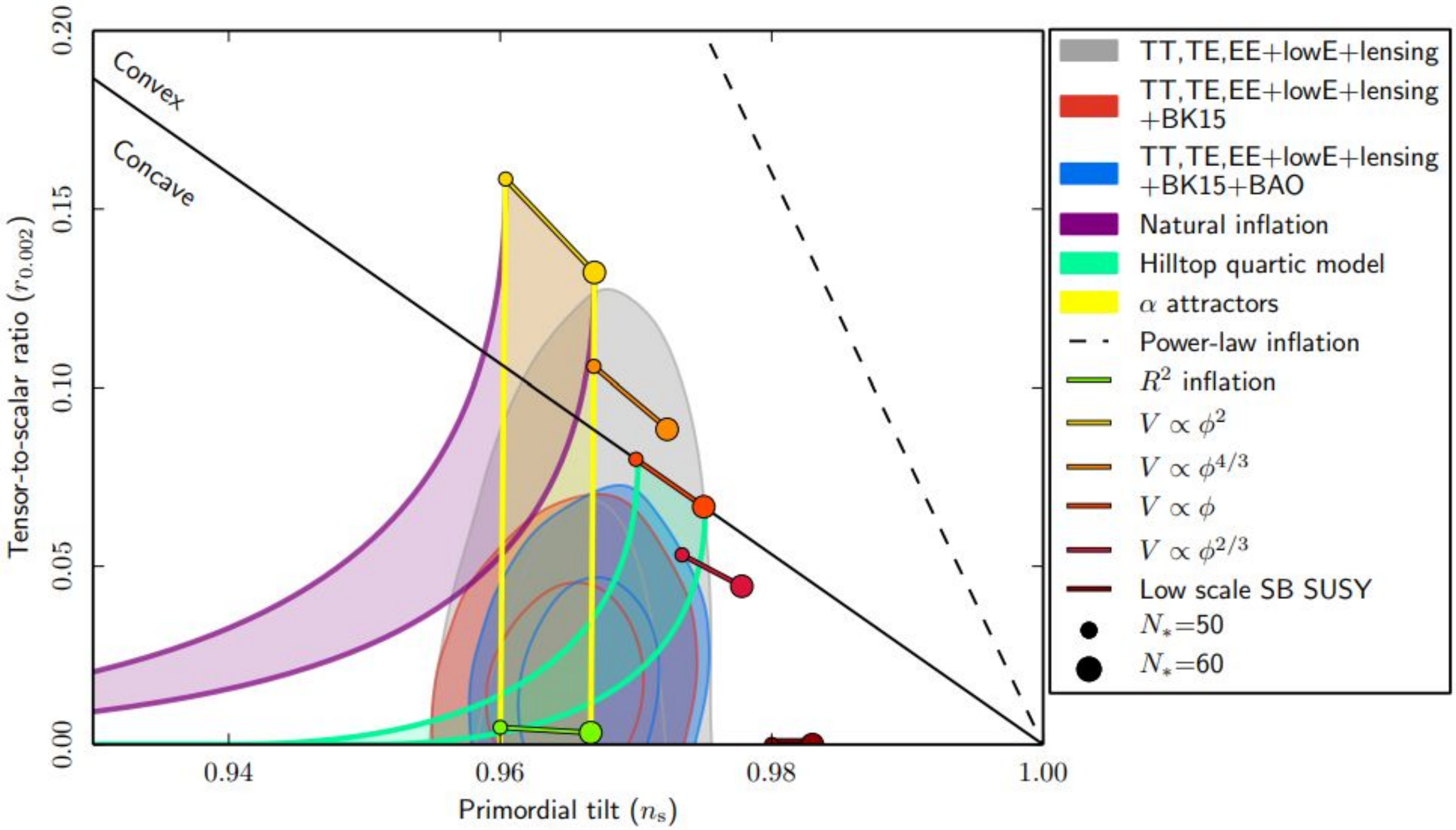

Fig. 8. Marginalized joint 68 % and 95 % CL regions for n_s and r at $k = 0.002\,\mathrm{Mpc}^{-1}$ from *Planck* alone and in combination with BK15 or BK15+BAO data, compared to the theoretical predictions of selected inflationary models. Note that the marginalized joint 68 % and 95 % CL regions assume $dn_s/d\ln k = 0$.

Conclusion

PICO: 21 frequency bands and for ⅘ sky models:

- if $r = 0$, $r < [1.3 \times 10^{-4}, 2.4 \times 10^{-4}]$, with 95% confidence levels → this would rule out simplest models of inflation that predict $r \approx 0.001$
- if $r = 0.003$, detected with confidence levels ~ 20σ after 5 years of mission

For high complexity model, mitigation of bias if aggregation of low dust regions →

- If $r = 0$, $r < 1.6 \times 10^{-4}$ with 95% confidence level

⇒ Strongest upper limits and detection predicted for any instrument

⇒ Need of a space mission to do this with a large frequency range and high sensitivity as PICO!

Sources of contamination: Polarized foregrounds and CMB lensing

- Even with this high sensitivity, contamination due to foregrounds!
- Foregrounds in polarization:

<u>Dust</u>

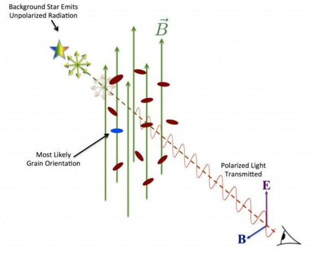

Credit: PASIPHAE

<u>Synchrotron</u>

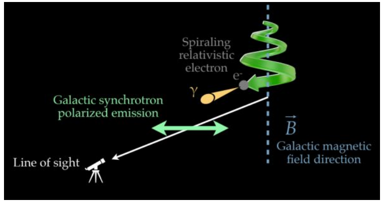

Credit: J. Aumont

<u>Anomalous microwave emission (AME)</u>

Correlated with thermal dust emission

Polarization not measured yet but predicted and modeled

in the sky models to 2%